The American Journal of Pathology, Vol. 175, No. 5, November 2009

DOI: 10.2353/ajpath.2009.090380

Cell Injury, Repair, Aging and Apoptosis

The Cellular Biology of Flexor Tendon Adhesion Formation

An Old Problem in a New Paradigm

Jason K.F. Wong,* Yin H. Lui,† Zoher Kapacee,† Karl E. Kadler,† Mark W. J. Ferguson,‡§ and Duncan A. McGrouther*

From Plastic Surgery Research, Faculty of Medicine and Human Sciences, the Wellcome Trust Centre for Cell-Matrix Research,† Faculty of Life Sciences, and the Faculty of Life Sciences,‡ University of Manchester, Manchester, United Kingdom, and Renovo Plc.,§ Manchester, United Kingdom.*

Intrasynovial flexor tendon injuries of the hand can frequently be complicated by tendon adhesions to the surrounding sheath, limiting finger function. We have developed a new tendon injury model in the mouse to investigate the three-dimensional cellular biology of intrasynovial flexor tendon healing and adhesion formation. We investigated the cell biology using markers for inflammation, proliferation, collagen synthesis, apoptosis, and vascularization/myofibroblasts. Quantitative immunohistochemical image analysis and three-dimensional reconstruction with cell mapping was performed on labeled serial sections. Flexor tendon adhesions were also assessed 21 days after wounding using transmission electron microscopy to examine the cell phenotypes in the wound. When the tendon has been immobilized, the mouse can form tendon adhesions in the flexor tendon sheath. The cell biology of tendon healing follows the classic wound healing response of inflammation, proliferation, synthesis, and apoptosis, but the greater activity occurs in the surrounding tissue. Cells that have multiple "fibripositors" and cells with cytoplasmic protrusions that contain multiple large and small diameter fibrils can be found in the wound during collagen synthesis. In conclusion, adhesion formation occurs due to scarring between two damaged surfaces. The mouse model for flexor tendon injury represents a new platform to study adhesion formation that is genetically tractable. ***(Am J Pathol 2009, 175:1938–1951; DOI: 10.2353/ajpath.2009.090380)***

The clinical problem of flexor tendon injuries can be complicated when healing results in adhesions forming between the tendon and the surrounding synovial sheath. Although difficult to predict following surgical repair, adhesions have long been accepted as a cause of restricted tendon movement. Recent clinical studies on 315 primary flexor tendon repairs reported that approximately 28% of flexor tendon repairs had a fair to poor functional recovery, likely to be attributable to adhesion formation.[1] The area where this is most problematic is known as "no man's land,"[2] or zone II,[3] where two tendons glide within a flexor tendon sheath in the fingers. The formation of adhesions leads to impairment of digit flexion through inhibiting normal tendon gliding. In an attempt to understand the pathophysiology of flexor tendon adhesions, a number of tendon healing concepts have been derived.

The concepts surrounding our current understanding of flexor tendon healing have remained unchallenged for several decades. In 1963, Potenza had hypothesized that adhesion formation was a requirement for blood vessel in-growth into the tendon.[4] This hypothesis supported the concept of *extrinsic healing* of tendon from the surrounding tissue. Matthews and Richards[5] showed that flexor tendon healing could occur in the absence of adhesions and attributed this to certain cell populations within tendon. This concept of healing, later termed *intrinsic healing,* was attributed to the activity of cells within the tendon. These observations were supported by a series of histological, *in vitro,* and ultrastructural studies. Injured intrasynovial tendon was shown to heal independently of adhesions in a synovial environment,[6] when explanted to

Supported by the University of Manchester/Renovo Lectureship, The Royal College of Surgeons of Edin, and Renovo Plc.

Accepted for publication July 23, 2009.

M.W.J.F. is co-founder and shareholder in Renovo Plc.

Supplemental material for this article can be found on *http://ajp.amjpathol.org*.

Address reprint requests to Mr. Jason K.F. Wong, Room 3.60 Stopford Building, Faculty of Life Sciences, University of Manchester, Oxford Road, Manchester. M13 9PT. E-mail: jason.k.wong@manchester.ac.uk.

culture[7] and when transplanted to different body sites in diffusion chambers.[8] It has been the concepts of intrinsic and extrinsic healing that have guided strategies to improve flexor tendon repair outcomes over the years. In the context of modern understanding of wound healing, these concepts of tendon healing are outdated and require revisiting. Many *in vivo* studies use mice as a reference model for studying mammalian systemic responses such as wound healing.[9] The benefits of such a system include low maintenance, rapid and easy breeding programs, and genetic versatility.[10] We have previously described the mouse hind paw anatomy and identified numerous similarities it has to the human hand.[11] Furthermore, we have shown that the mouse digit can be used as a model for studying tendon injury through using a single grasping suture technique.[12] Adhesion formation has been demonstrated in allograft and autograft studies in a murine flexor tendon model.[13] The demonstration of intrasynovial flexor tendon adhesion formation in the clinically important "no man's land" of the digit has yet to be shown in a mouse model.

The development of an adhesion model would enable the quantification of adhesion formation and would also benefit the analysis of the cellular processes involved. The model may be used in developing strategies aimed at preventing adhesion formation.

Many studies have investigated independently the processes involved in flexor tendon healing, including inflammation,[14] proliferation,[15] collagen synthesis,[16] vascularization,[17] and apoptosis.[18] We have attempted to observe all these aspects of the tendon healing response to give a detailed overview of the healing process.

This study aimed to give a broad understanding of the process of adhesion formation, using three-dimensional (3D) cellular mapping to investigate the interplay of cellular repair.

Materials and Methods

Animals

All animal procedures were approved by the Local Ethical Review Process at the University of Manchester and complied with the relevant licenses approved by the UK Home Office on the Care and Use of Laboratory Animals.

The *in vivo* study used the deep digital flexor tendons of both the hindpaws in male C57/BL6 mice between 10 and 12 weeks (25 to 30 g) of age.

Wounding Model

Surgery was performed using a standard mouse general anesthetic protocol, which entailed induction using 4% isoflurane (Abbott, UK) and 4 L/minute oxygen driver. Once induced, the anesthesia was maintained using 2% isoflurane with 2 L/minute oxygen driver and 1.5 L/minute nitrous oxide. The left hind limb was cleaned with 70% ethanol, and a bloodless operative field was secured through application of a tourniquet, using dressing elastic to the popliteal fossa. Surgical procedures were performed with the aid of a Leica MZ7.5 Operating microscope (Leica Microsystems, Germany) at ×10 to ×40 magnification.

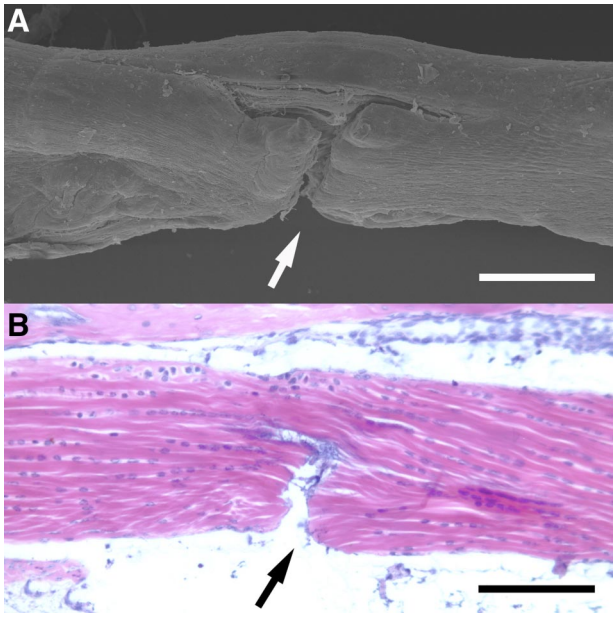

Figure 1. Partial laceration (PL) of mouse digit flexor tendon. **A:** Scanning electron microscopy of partially lacerated tendon. Approximately 50% of the fibers divided (**arrow**). **B:** Basic histology (H&E staining) of partially lacerated tendon (**arrow**). Scale bars = 200 μm.

Forty-four mice sustained partial lacerations (PL) to the third and forth digits of each hindpaw. The deep digital flexor tendon was first exposed through a transverse skin incision and a standardized PL was performed in between the A1 and A3 pulley over the proximal phalanx.

The PL aimed to divide approximately 50% of the tendon fibers. This injury was performed using Cohen Vannas microscissors (Fine Science Tools, UK) by freehand under magnification. Validation of the reproducibility and variability of the injury was assessed by performing the same injury in mouse cadaver tissue and analyzing the depth of injury using scanning electron microscopy (Figure 1, A and B). Following PL, the skin was closed over the tendon wound with a single 10/0 polyamide suture (Braun Medical, Germany). The tourniquet was removed and hemostasis maintained by the application of mild pressure. The hindpaw was cleaned with 0.9% saline.

Following PL of the tendon on the left hind limb, a further skin incision was made just distal to the ankle joint and the common deep and superficial flexor tendons and a proximal tenotomy (PT) was performed. This involved completely dividing the deep and superficial digital tendons. The proximal ends of these tendons were buried to prevent the distal and proximal tendon ends from approximation. The skin was then closed with two interrupted 10/0 polyamide sutures (Braun Medical, Germany). The right hind limb did not have a proximal tenotomy performed, but only a PL in the tendon (PL only group). Once the mice had recovered from the effects of anesthesia, they were carefully monitored for any signs of distress. Daily weights were recorded to identify any subtle dis-

Table 1. Antibodies, Pretreatments, Reagents, and Controls Used for Labeling Samples

Antibody	Pretreatment	Blocking solution	Primary incubation	Secondary incubation	ABC	Substrate	Control tissue
BrdU (Abcam)	10 minutes in 4 mol/L HCL, 5 minutes in borate buffer	1% rabbit serum for 1 hour at room temperature	1:200 for 1 hour 37°C	1:200 rabbit anti-rat biotinylated IgG for 15 minutes room temperature	Yes	DAB	Spleen
Hsp47 (Stressgen)	None	MOM block for 1 hour room temperature	1:200 for 1 hour 37°C	MOM kit 2 IgG for 10 minutes room temperature	Yes	DAB	Skin wounds
α-SMA (Abcam)	None	2.5% goat serum for 1 hour room temperature	1:200 for 1 hour 37°C	ImmPRESS kit for 30 minutes room temperature	No	DAB	Spleen
TUNEL (Roche)	30 minutes in Tris HCL	None	2:3 for1 hours 37°C	1:2:1 Sheep serum: PBS: POD kit for 30 minutes room temperature	No	DAB	Large intestine
CD45 (BD pharmingen)	None	1% rabbit serum for 1 hour room temperature	1:100 for 1 hour 37°C	1:200 rabbit anti-rat biotinylated IgG for 30 minutes room temperature	Yes	DAB	Spleen
F4/80 (Serotec)	None	1% rabbit serum for 1 hour room temperature	1:200 for 1 hour 37°C	1:200 rabbit anti-rat biotinylated IgG for 30 minutes room temperature	Yes	DAB	Spleen
Ly6G (BD pharmingen)	None	1% rabbit serum for 1 hour room temperature	1:200 for 1 hour 37°C	1:200 rabbit anti-rat biotinylated IgG for 30 minutes room temperature	Yes	DAB	Skin wounds

ABC, avidin-biotin complex; MOM, mouse on mouse; POD, peroxidase detection; DAB, diaminobenzidine.

tress. Following injury, the mice were allowed to mobilize freely and euthanized at 1, 3, 5, 7, 10, 14, 21, 28, 56, 84, and 112 days. These time points were selected to give a broad and detailed time course of the healing process, according to previous wound healing studies.[19] This equated to four mice collected per time point with both hind limbs being assessed for adhesion formation. Six mice with unwounded hindpaws were used as controls. Four hours before tissue collection, each mouse had 10 μl/g of 5-bromo-2-deoxyuridine (BrdU, GE Health Care, UK) injected into their peritoneal cavity.

Tissue Processing

The hind limbs were collected and immediately immersed in zinc fixative[20] for 48 hours at 4°C. The third digit of each limb was dissected free and decalcified in 20% EDTA for 15 days, with solution changes every 5 days. Following this process, the decalcified third digit was tissue-processed. The fourth digit soft tissue from each hind limb was filleted off the bone and stored in 70% ethanol for 48 hours before tissue processing. Great care was taken to prevent any shear or traction to the tendon on dissection. All tissue was tissue processed using a Tissue-Tek Vacuum infiltration Processor (Bayer Diagnostics, Newbury, UK) and embedded in paraffin wax. Serial sections, 7 μm thick, were cut from the paraffin embedded blocks. These sections were mounted onto 4% 3-aminopropyltriethoxysilane and 10% poly-L-lysine dual-coated slides, followed by drying at 37°C for 24 hours. Four sections were positioned on each slide and every other slide was stained with H&E Y stain (Raymond A Lamb, UK).

Immunohistochemistry

For the third digit, three sections from around the central slide were antibody stained on independent sections for BrdU (marker for proliferation), heat shock protein 47 (Hsp47 or "collingin," marker for type I collagen synthesis), α smooth muscle actin, (α-SMA, marker for pericytes and myofibroblasts), and terminal deoxynucleotidyl transferase biotin-dUTP nick end labeling (TUNEL marker for DNA fragmentation/apoptosis). The fourth digit was serially sectioned and on independent sections, labeled with CD45 (common leukocyte antigen marker), F4/80 (activated macrophage marker), and Ly6G (neutrophil marker) in triplicate per mouse digit (see Supplemental Figure S1 at *http://ajp.amjpathol.org*). Immunoperoxidase techniques were standardized following initial dilution studies to establish optimal dilutions and conditions for all primary antibodies. For mouse monoclonal antibodies a specific mouse on mouse kit was used. For rat monoclonal antibodies, a standard rabbit anti-rat biotinylated secondary antibody was used and amplified using the Elite ABC kit. For rabbit polyclonal antibodies, the rabbit ImmPRESS biotinylated kit was used. These kits were used as recommended in the manufacturer's guidelines (Vector Laboratories, Peterborough, UK). The TUNEL kit (Roche) was used with peroxidase conversion, which allowed for assessment by 3,3′diaminobenzidine substrate staining. Antibody labeling of samples was undertaken using the protocol described above (Table 1.). Samples were washed twice for five minutes using 0.1% Tween (v/v) in PBS between each step of the protocol.

Images of the stained sections of the zone II region of the digit, where the deep and superficial flexor tendons

glide within the synovial sheath, were obtained using a Leica DMRB Microscope (Leica Mircosytems, Germany) with an attached Spot camera (Diagnostic Instruments Inc.). Images were processed on a silicon graphics workstation (SGI, UK) and saved using Spot 4.5 software (Diagnostic Instruments, Inc.) as .tiff files.

Image Analysis

The slide that represented the center of the digit was identified and two slides to each side of the center slide, each slide 28 μm apart, were analyzed for mean sheath space, flexor tendon area, the mean tendon diameter, and the length of the adhesion. The measurements were made by image analysis software (Image Pro Plus version 4.5, Media Cybernetics) following calibration.

With analysis based around five stereological aligned sections, it was possible to calculate the area of adhesion, the volume of the deep digital flexor tendon and the volume of sheath space based on Cavalieri principles.[21] Image acquisition of the tendon and subcutaneous tissues (ST) cellular variables was performed on three sections 28 μm apart. Six fields of view were selected for calculating cellularity and cellular expression of antibodies. Cell counts were performed on three fields of view for the tendon (see Supplement Figure S2, A–C at *http://ajp.amjpathol.org*) and three fields of view for the sheath and ST (see Supplement Figure S2, D–F at *http://ajp.amjpathol.org*) on three different sections. The total number of fields analyzed per digit was 18 fields (nine tendon and nine sheath/subcutaneous tissue fields). Each field measured 50 μm by 200 μm. Cells were counted using the Image Pro Plus 4.5 software (Media Cybernetics). The mean value of cellular expression for each digit was calculated for tendon and for ST and expressed as cells/mm^2.

Three-Dimensional Reconstruction and Cellular Mapping

Three-dimensional reconstruction of electron microscopic topography using Reconstruct has previously been described.[22] We have applied the same methodology to serial sectioned and aligned immunohistochemical samples. Briefly, serial sectioned histology and immunohistochemical image files were calibrated and imported as .tiff files into the Reconstruct program. Wire maps were produced by tracing individual structures such as tendon, blood vessels, and the STs. The area of adhesion was also mapped by outlining the point of contact between tendon and sheath for ease of identification on the reconstructed images. Distances between each image were calibrated and individual cells were mapped according to their stereological position and reproduced using the program's sphere option. Boissonnat surface shading and color selection and transparency features were introduced post processing of the 3D reconstruction. Tendon was highlighted in orange, the adhesion was light blue, and the subcutaneous tissue was purple. CD45 positive (+) cells were labeled in pink, Ly6G+ cells in yellow, and F4/80+ cells in white. BrdU expression was mapped in red, Hsp47+ cells were mapped in green, α SMA+ vessels were mapped in red, and TUNEL expression was mapped in blue.

Scanning Electron Microscopy

Tendon samples were fixed in 2.5% gluteraldehyde (Taab, UK) in 0.1 M/L sodium cacodylate buffer at pH 7.4 for 24 hours. Samples were then washed three times for 10 minutes in 0.1 M/L sodium cacodylate buffer, before transfer to 1% osmium tetroxide (Johnson and Mathey, UK) in 0.1 M/L sodium cacodylate buffer at pH7.4 for 2 hours. Samples were then washed in distilled water three times for 10 minutes and then dehydrated through graded ethanol series, with 30 minutes in each 50%, 70%, 90%, 100%, 100%, and 100%, before critical mass drying in an Emitech k750 (Kent, UK) critical point dryer. Samples were then mounted onto stubs with double-sided sticking pads and sputter coated with gold, set at approximately 15 nm thickness. Samples were then viewed under a Cambridge 300 scanning electron microscope.

Transmission Electron Microscopy

Samples were prepared for electron microscopy as described previously.[23] Briefly, samples of unwounded mouse digital flexor tendon, embryonic mouse tail, and mouse digital flexor tendons, which had been wounded 3 weeks earlier, were fixed in 2% glutaraldehyde in 100 mmol/L phosphate buffer, pH 7.0, for 30 minutes at room temperature. The tails were then diced and post-fixed for 2 hours at 4°C in fresh fixative. After washing in 200 mmol/L phosphate buffer, the samples were fixed in 1% glutaraldehyde and 1% OsO_4 in 50 mmol/L phosphate buffer, pH 6.2, for 40 minutes at 4°C. After being rinsed in distilled water the samples were stained *en bloc* with 1% aqueous uranyl acetate for 16 hours at 4°C, dehydrated, and embedded in Spurrs' resin. Ultra-thin sections, ~60 nm thick, were cut for normal transmission electron microscopy and were collected on uncoated copper 200 grids. Serial sections were taken and placed on formvar-coated copper 1000 μm slot grids, stabilized with carbon film. All sections were subsequently stained with uranyl acetate lead citrate, and examined using a Philips BioTwin transmission electron microscope (Phillips Electron Optics, The Netherlands). Images were recorded on 4489 film (Kodak, UK) and scanned using an Imacon Flextight 848 scanner (Hasselblad).

Statistics

Mean values were calculated using SPSS 15.0 (SPSS Inc, Chicago, USA) and expressed with the SE of mean in brackets (± SEM). The changes in cellularity seen at different time points were tested for significance using one way analysis of variance and further analyzed using a Tukey post hoc test. Paired *t*-testing of data was performed between PL only, and PL and PT groups. Paired

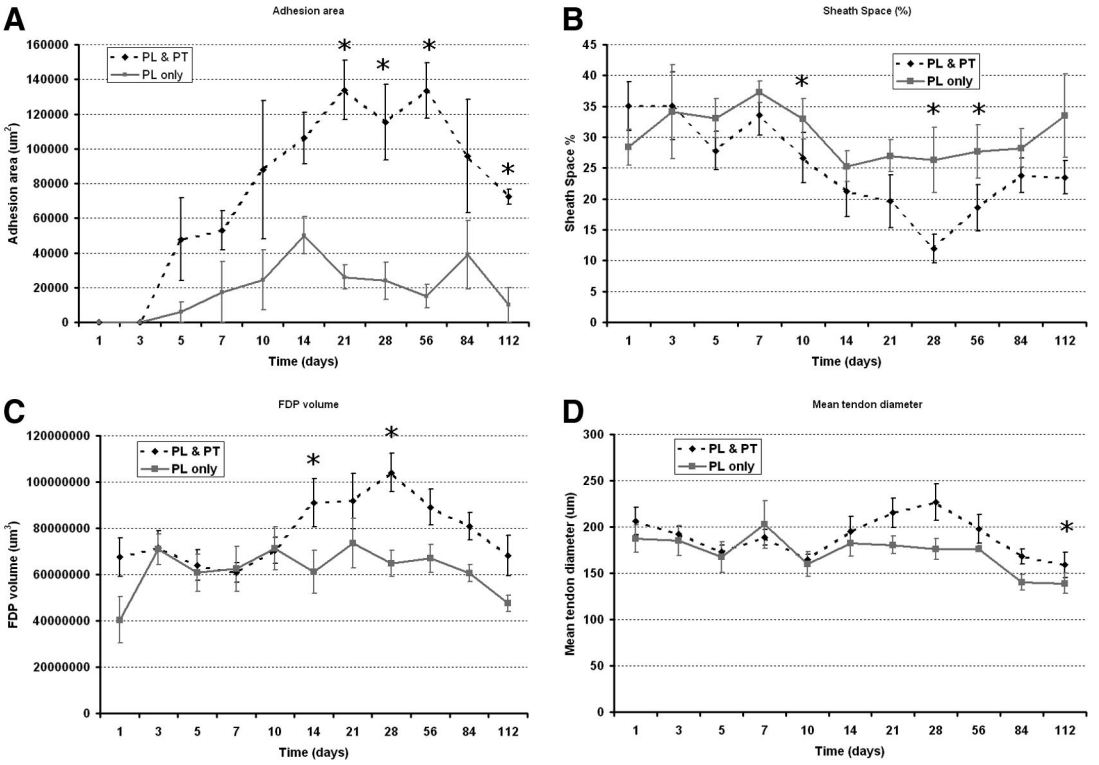

Figure 2. Temporal dimension changes comparison between mobilized and immobilized injured tendons. Partial laceration (PL)/mobilized non-adhesion forming model (solid line) and partial laceration and proximal tenotomy (PL and PT)/immobilized adhesion model (dotted line) observed over 112 days. **A:** Change in size of adhesion. **B:** Sheath space obliteration. **C:** Flexor digitorum profundus (FDP) tendon volume changes. **D:** Mean tendon diameter. Significant differences between PL and PL and PT, $*P < 0.05$. Error bars denote SEM.

t-testing was also performed for tendon and ST differences. In all cases, the *P* value was considered significant if below 0.05.

Results

Validation of the Rodent Model

The mean depth of injury induced by the standardized 50% laceration technique was analyzed using scanning electron microscope images. The mean depth of injury involved 50.4% (± 1.16) of the tendon diameter, based on ten mouse tendons, indicating the injury method was highly reproducible. From the serially sectioned histology samples, the central slide consistently showed that the PL involved 50% of the tendons diameter.

Adhesion Formation Is Propagated by Immobilization of the Digit

In total 34/44 (77.3%) digits from the PL and PT limbs formed adhesions, as compared with only 25/44 (56.8%) digits from the PL only group. Few definite adhesions were observed before 3 days. Data from day 10 onwards showed 27 of the 28 mice (96.4%) that had PL & PT formed localized tendon adhesions. The overall area of adhesion formed was shown to be significantly less in the PL only digits ($P < 0.001$) when performing paired comparisons with the PL and PT contralateral limb. When comparing the adhesion formation process at individual time points, we showed that at 21 days ($P = 0.01$), 28 days ($P = 0.05$), 56 days ($P = 0.01$), and 112 days ($P = 0.004$) post injury, adhesion formation was significantly greater in PL and PT limbs than their PL only limbs (Figure 2A). The sheath space was significantly reduced in PL and PT limbs, as compared with PL only limbs on day 10 ($P = 0.017$), day 28 ($P = 0.022$), and day 56 ($P = 0.02$) (Figure 2B). Tendon volume was significantly more in PL and PT limbs on day 14 ($P = 0.046$) and day 28 ($P = 0.004$) (Figure 2C) and tendon diameter was only significantly greater in PL and PT limbs on day 112 ($P = 0.033$) (Figure 2D).

Histological Changes over 4 Months

As the study focused on adhesion formation, the histological observations were made of the PL and PT model.

Following injury to the ST and tendon, there was a noticeable cellular response around the point of injury. The cellular infiltrate was low at 3 days, and there was gradual swelling of both the subcutaneous tissues and the tendon, which brings the surfaces of tendon and ST into contact (Figure 3A and B). The adhesion gradually increased in cellularity and reached a maximum area of 133,826 μm^2 (± 17,002) at 21 days (Figure 3C). The sheath space was reduced following injury and at its smallest at 28 days (11.94% [± 2.31]). After day 56, the adhesions gradually reduced in cellularity together

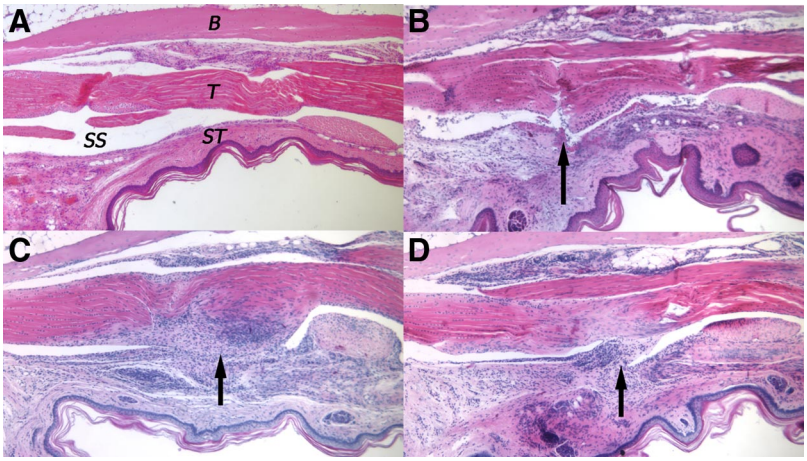

Figure 3. Basic histology of adhesion development in mouse flexor tendon. **A:** Unwounded flexor tendon within flexor sheath. T = tendon, ST = subcutaneous tissue, SS = sheath space, and B = bone. **B:** Day 3 wounded tendon. The **arrow** indicates location of partial laceration. Tendon and subcutaneous tissue were thicker due to tissue swelling and cell infiltration. **C:** Day 21 wounded tendon. The **arrow** indicates adhesion formation at interface between tendon and sheath. The adhesion is very cellular and clearly has different matrix staining to unwounded tendon. **D:** Day 112 wounded tendon. The **arrow** indicates the adhesion. The adhesion is more sparsely populated with cells and the interface between the tendon and sheath persists.

with the volume and diameter of the tendon (Figure 2C). By day 112 the area of adhesion was significantly less (72,324 μm^2 [± 4,402]) and appeared fibrous (Figure 3D).

Expression of Cellular Markers for Wound Healing

Cell counting of the labeled cells in the tendon and surrounding ST was quantified separately. The pattern of cell activity occurred in accordance with the classical phase response of wound healing, ie, inflammation, proliferation, and synthetic phases. In addition we investigated the vascularization and apoptotic changes during these phases.

Inflammatory Cells Predominate in the Surrounding Tissues in the Early Phases of Healing but Appear in Tendon during the Remodeling Phase

Within 24 hours of injury to the mouse flexor tendon, there was a massive influx of CD45+ labeled cells in the surrounding tissues and in the sheath space. Concurrent Ly6G staining demonstrated that the majority of these cells were neutrophils (Figure 4). Ly6G expression rapidly diminished after 24 hours and was absent by 5 days (Figure 4B). Cellular expression of CD45 remained elevated with small peaks at seven days and 14 days postinjury (Figure 4A). There was little expression of CD45 in the tendon substance until day 14, which coincided with increasing expression of F4/80 in the tendon. F4/80 expression in the tendon was greatest at 21 days. The significant peaks in expression of F4/80 occurred on day 3 ($P = 0.005$), day 7 ($P = 0.025$), and day 14 ($P = 0.014$) in the ST, which coincided with peaks in expression of CD45 on days 7 and 14 (Figure 4C). CD45 expression in the tendon and ST gradually reduced to baseline levels by 112 days. F4/80 and Ly6G expression was low after day 28 (Figure 4). CD45+ cell expression in relation to Ly6G and F4/80 expression showed a similar distribution pattern but many CD45+ cells in the ST did not overlap in expression with F4/80 of Ly6G (Figure 5).

Proliferative Activity Occurs in Both the Surrounding Tissues and Tendon but Is Greater in the Surrounding Tissues

Labeling of BrdU immediately following injury was clearly diminished in the proliferating basal layer of the epidermis. BrdU labeling increased rapidly by 3 days in the ST (Figure 6A). In the tendon there was also evidence of cellular proliferation in the zone of injury and also on the dorsal aspect of the tendon in the vinculum. By day 7, there was a second peak of proliferative activity in both the tendon and ST. BrdU labeling remained elevated for up to 56 days before returning to baseline levels. The pattern of proliferation activity in both the tendon and ST were fairly similar although levels of expression were significantly higher in the ST on day 3 ($P = 0.008$), days 5 ($P = 0.002$), day 7 ($P = 0.017$), and day 10 ($P = 0.01$) (Figure 6A). Three-dimensional cellular mapping showed that proliferation activity was greatest in the area of adhesion and showed the distribution of BrdU+ cells was greater in ST on day 7. By day 21, the distribution of BrdU+ cells was greater in and around the site of adhesions (Figure 7).

Collagen Synthesis in Tendon and Subcutaneous Tissue Are Temporally Different

Expression of Hsp47 was evident from 3 days following injury, with expression being predominating in the ST (Figure 6B). The mean synthetic activity in the sheath reached a peak at 10 days, at 714.2 cells/mm^2 (± 159.83) and synthetic activity in the tendon at this point was significantly lower, at 203.4 cells/mm^2 (± 42.67) ($P = 0.024$). By day 21, the peak in Hsp47 expression was 730.5 cells/mm^2 (± 73.34) and was significantly greater than levels in the ST, which was calculated at 452.35 cells/mm^2 (± 134.54) ($P = 0.026$). Hsp47 peak activity in

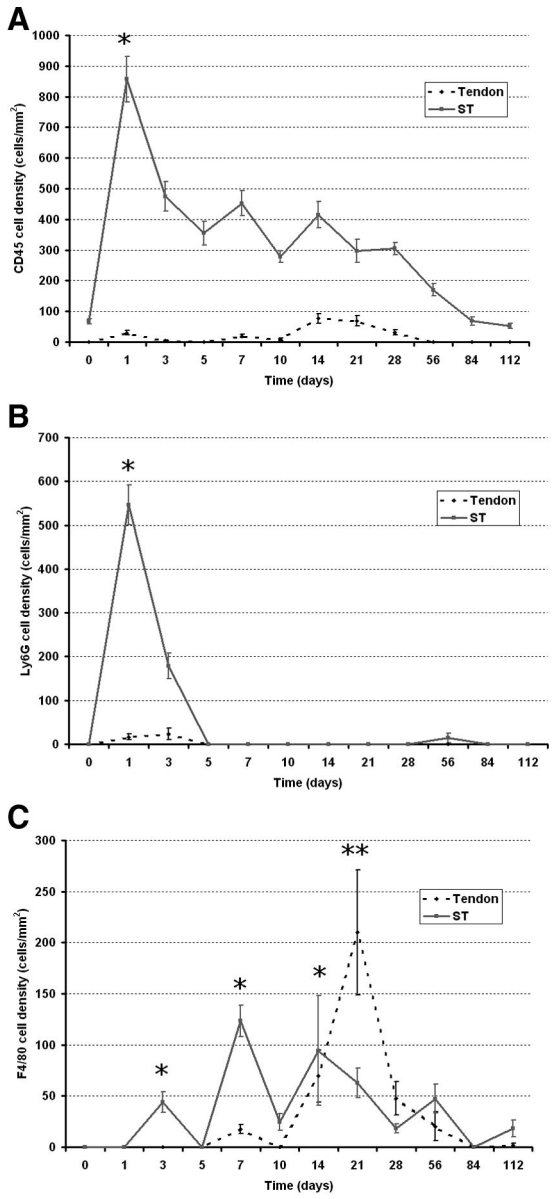

Figure 4. Temporal inflammatory cell (CD45, F4/80, and Ly6G) activity changes in immobilized adhesion model (PL and PT). The dotted line graph represents activity in the tendon and the solid line graph represents activity in the subcutaneous tissues. **A:** CD45 activity. Peaks at one day and gradually declines. Note small peak in activity in tendon at 14 days. **B:** Ly6G activity. There is marked expression at day 1 that rapidly diminishes by day 5. Very little expression was observed in the tendon substance. **C:** F4/80 activity. Significant peaks in the subcutaneous tissue on day 3, day 7, and day 14 are indicated by **asterisks**. Note marked increase in activity in tendon on day 21, which was significant $^{**}P < 0.05$. Error bars denote SEM.

tendon and ST was offset suggesting that the onset of activity in the tendon arose after a latency period, but there was overlapping synthetic activity with both tissues expressing high levels of Hsp47 at around 14 days. This was reflected in the changes seen on cellular mapping (Figure 7). Activity was high in the ST as seen on day 7. By day 21 there was florid Hsp47 activity in the area of adhesion and tendon.

Pericyte and Myofibroblast Activity Predominates in the Subcutaneous Tissue and Not Tendon

Using α-SMA as a marker for pericytes and myofibroblasts, we were able to investigate the vascularity of the tissues following injury. There was no expression of α-SMA expression in tendon throughout the time course. The ST did show marked changes in α-SMA over the 112 days of study. The greatest peak of α-SMA expression was seen at day 7, and this corresponded to both high levels of pericyte expression and myofibroblast activity in the contracting ST wound (Figure 6C). At day 10, the expression of α-SMA was only associated with the vasculature, but continued to show elevated expression over the course of 112 days. Three-dimensional cellular mapping indicated that the blood vessels collapsed and could not be seen on the first day after injury. By day 7, vascularity increased and small vascular islands could be seen to increase in volume over the course of 112 days. The vascular anatomy was gradually restored forming long channels of α-SMA lined vessels (Figure 7).

Cell Death Gradually Increases toward the End of Healing

Following injury, in the immediate vicinity of the lacerated tendon and ST wound there was localized and marked staining of TUNEL+ cells followed by a gradual trend of increased expression over the course of 84 days, with a peak at 84 days post-injury. TUNEL staining followed a similar pattern in tendon and the ST, although more apoptotic cells were seen in the ST. Three-dimensional mapping of cells indicated the distribution of TUNEL+ cells were predominantly in the ST. As numbers of CD45+ cells decreases there appeared to be a concurrent increase in the number of TUNEL+ cells in the same areas of distribution (Figure 4A and Figure 6D). This inverse association between CD45 and TUNEL labeling was shown to be significant ($P = 0.004$).

Fibripositor Cell Phenotypes Are Found in the Collagen Synthesizing Tendon Wound

Tendon fibroblasts in normal unwounded tendon had a stellate shape on cross section with smooth, concave cell membranes and thin cell cytoplasm. The cytoplasm at high magnification showed no evidence of fibrils within the cytoplasmic membranes. Fibrils that make up the matrix were large diameter with few interspersed smaller diameter fibrils (Figure 8A). Embryonic tendon fibroblasts had long cytoplasmic membranes and small fibrils with small fibrils enclosed in cytoplasmic processes, which have previously been termed 'fibripositors'[23] (Figure 8B). In adhesion forming tendon wounds after 21 days, there were two distinct cell phenotypes observed. The first cell type was a large cell with multiple cytoplasmic protrusions, which were seen to enclose large and small diameter fibrils or even multiple fibrils (Figure 8C). This cell

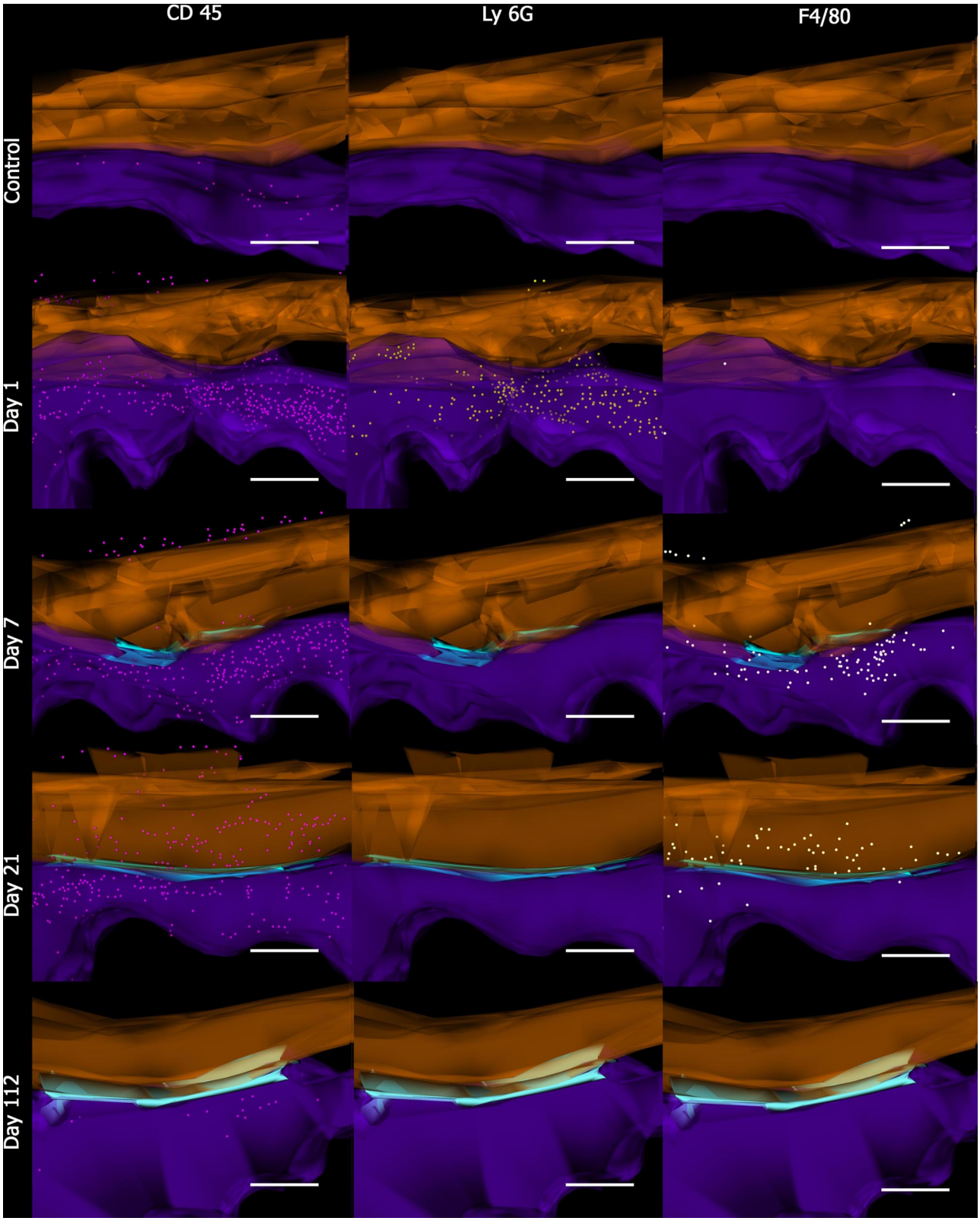

Figure 5. Three-dimensional cellular mapping of inflammatory cell activity. Images are of 3D reconstructions with spatial and temporal representations of inflammatory cells during the tendon adhesion forming process. Images of controls, day 1, day 7, day 21, and day 112, after partial laceration and immobilization are represented along the *y* axis. CD45+ cells (pink), Ly6G+ cells (yellow), and F480+ cells (white) are represented along the *x* axis. Tendon is represented in orange and subcutaneous tissue (ST) is represented in purple. The adhesion is represented in light blue. Scale bar = 200 μm.

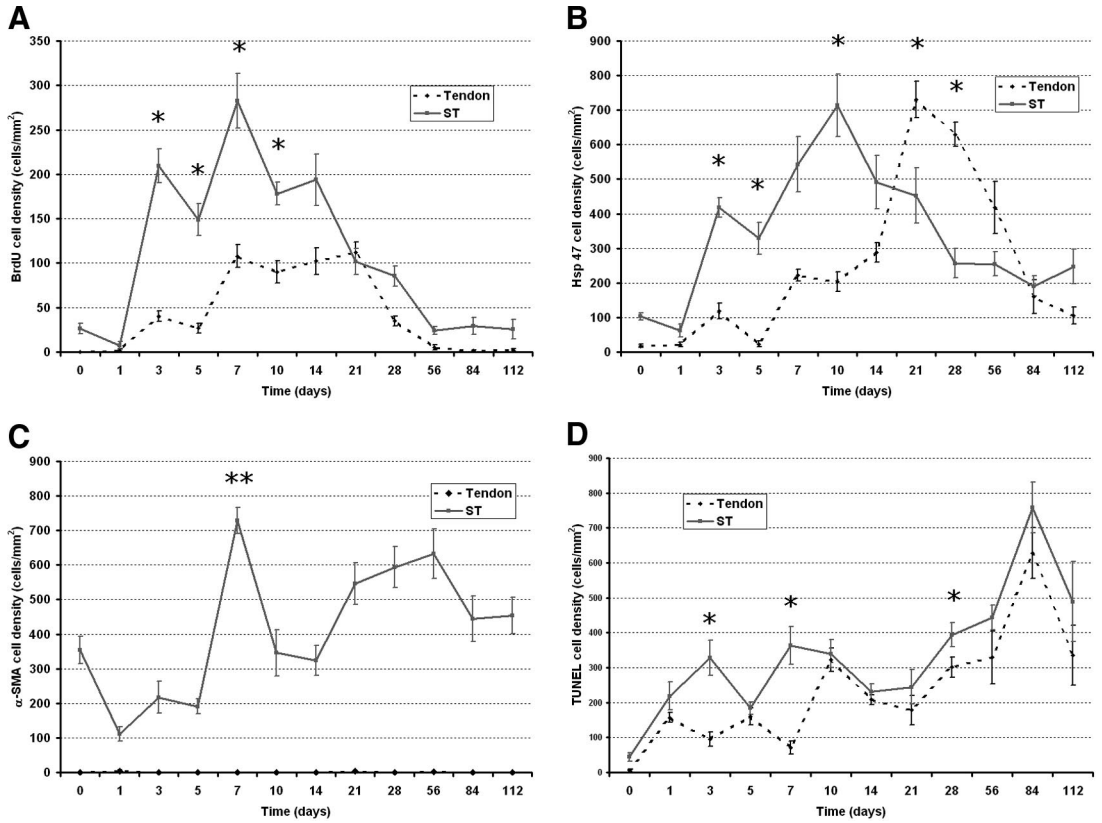

Figure 6. Temporal cellular activity changes in immobilized adhesion model (PL and PT). The dotted line graph represents activity in the tendon and the solid line graph represents activity in the subcutaneous tissue (ST). **A:** BrdU activity as a marker of cell proliferation. **B:** Hsp47 activity as a marker of type 1 collagen synthesis. **C:** α-SMA expression as a marker for pericytes and myofibroblasts. **D:** TUNEL expression as marker for apoptosis. Significant differences between tendon and ST are indicated by **asterisks** except **C**, where all values are significantly different ($P < 0.05$). **Double asterisks** in graph (**C**) indicates expression of both myofibroblasts and pericytes. Error bars denote SEM.

phenotype showed enlarged endoplasmic reticulum and Golgi apparatus. The second cell phenotype was similar to those seen in developing tendon, with small cytoplasmic protrusions and small fibrils being deposited by 'fibripositors' (Figure 8D). The number of fibripositors was greater than those seen in development.

Discussion

Injury to flexor tendons through trauma or surgical manipulation can result in problematic tendon adhesion formation. This observation led pioneers of hand surgery such as Bunnell[24] to highlight the importance of an atraumatic technique and minimal handling in tendon surgery. Adhesion formation affects the normal tendon gliding that occurs within a narrow flexor tendon sheath. Few studies have reported that all tendon lacerations also include significant surrounding tissue trauma and in considering the whole healing process, flexor tendon studies should assess all tissues involved.

Fiberoptic studies of surgical patients have demonstrated that the tendons, sheath, STs, and skin glide across each other in vascularized interconnecting tissue planes during finger flexion, with scarring of these planes affecting the fingers ability to flex.[25] The investigation of the healing activity in these different tissue types is often difficult, due to the dimensions of the chosen model, hence previous studies used indirect methods of measurement such as pull out studies and range of movement studies.[26,27] In 1960, Lindsay and Thomson[28] had shown immobilization was key to adhesion formation after systematic wounding of the tendon, sheath, skin, ST, and vinculum complex. These studies showed damage to the skin, sheath, STs, and vinculum alone was insufficient to form adhesions. We have found that a clean, sharp laceration though the skin and sheath, along with a partial tendon laceration and relative immobilization, was sufficient for a localized tendon adhesion to form in mice. We have mapped out the cellular interactions of the adhesion forming process.

A key factor in the development of adhesions in this model was immobilization. Without a PT, few tendon adhesions formed. Keeping the damaged tendon and damaged ST (including the sheath) in relatively close approximation appears to be required for adhesions to form. This has been the key factor in previous animal models where groups have used casting,[4] suture anchorage,[29] neurectomy,[30] or proximal tenotomy and casting,[31] to promote adhesion formation. Clinical studies advocate early active mobilization[32] to improve tendon excursion, which continues to be the mainstay of management in hand therapy clinics for flexor tendon repairs.

Immediately following injury, it was evident that the cellular reaction from the ST would play a significant role

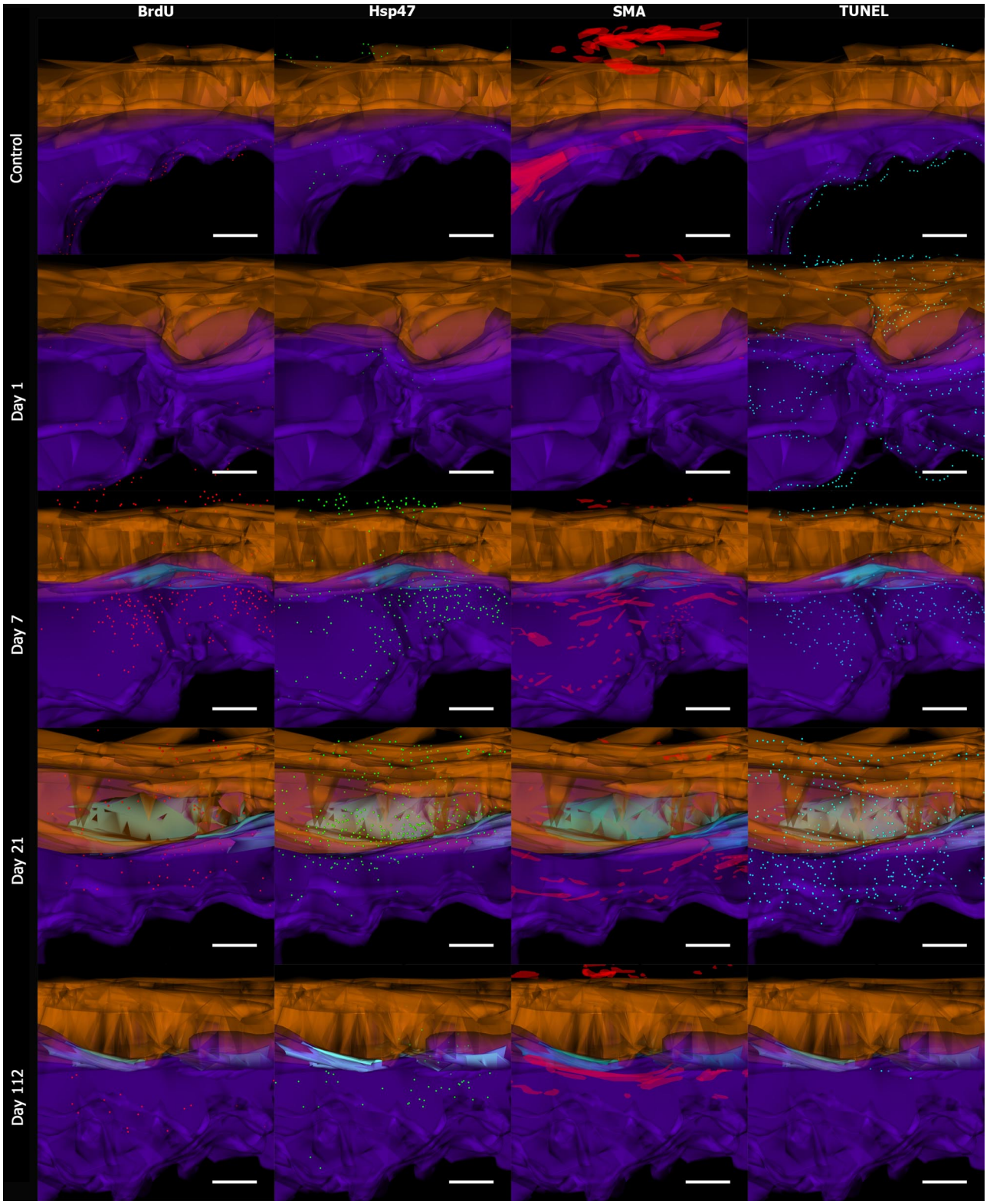

Figure 7. Three-dimensional cellular mapping of cell activity. Images are of 3D reconstructions with spatial and temporal representations of proliferating, synthesizing, myofibroblast/pericytes, and apoptosing cells during the tendon adhesion forming process. Images of controls, day 1, day 7, day 21, and day 112 after partial laceration and immobilization are represented along the *y* axis. BrdU+ cells (red), Hsp47+ cells (green), α-SMA+ vessels (red), TUNEL+ cells (blue) are represented along the *x* axis. Tendon is represented in orange, and subcutaneous tissue (ST) is represented in purple; adhesion is represented in light blue. Scale bar = 200 μm.

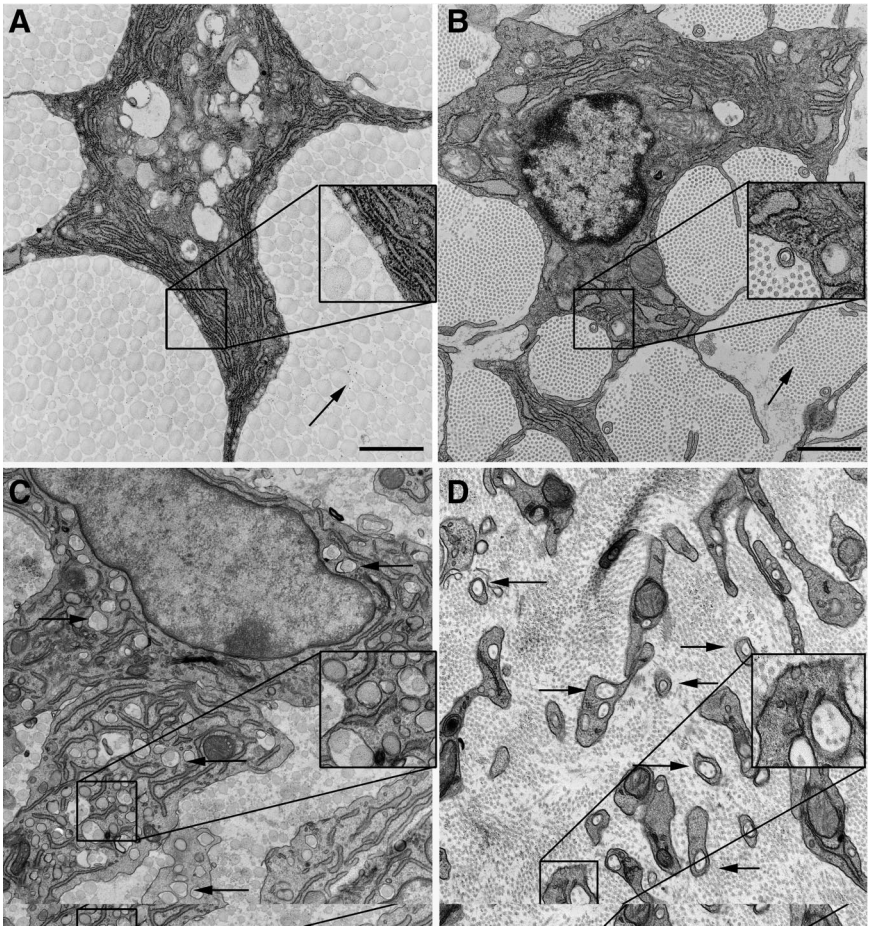

Figure 8. Transmission electron microscopy of cells in tendon wound. **A:** Normal unwounded adult mouse tendon. Note large diameter fibrils outside smooth cytoplasm of cell (**arrow**). Box = magnified × 2 cell border and fibrils. **B:** Embryologic mouse tendon 15 days gestation. Note small diameter fibrils (**arrow**). Box = magnified × 2 fibril in small cytoplasmic protrusion or "fibripositor." **C:** Mouse tendon 3 weeks after injury. Cell showing large diameter fibrils within cytoplasmic protrusions surrounded by heterogeneous fibril debris (**arrow**). Box = magnified × 2 large and small diameter fibrils in large cytoplasmic protrusion or "megapositor." **D:** Mouse tendon 3 weeks after injury. Cell showing small diameter fibrils within cytoplasmic protrusions. Similar phenotype to embryonic tendon with 'fibripositors' (**arrows**). Box = magnified × 2 multiple small diameter fibrils in cytoplasmic protrusions.

in dictating how the tendon was to heal. In this respect, *in vitro* tendon healing studies would provide an inaccurate representation of the pathobiology. The benefits of using a murine model include the ability to observe the systemic response to trauma in a mammalian system, which is genetically tractable. Furthermore, the miniaturization of the clinical problem allowed for tendon, sheath, ST, skin, and bone to be assessed on one sample image. This has benefits over previous models in larger animals, where only small sample areas of either tendon or sheath could be analyzed due to the logistics of sampling large blocks of tissue. The murine platform for flexor tendon healing represents a marked refinement and improvement from previous tendon adhesion models.

Our study has shown that flexor tendon injury followed a typical wound healing response involving overlapping phases of inflammation, proliferation, synthesis and remodeling, including apoptosis/necrosis and vascularization.

Our tendon adhesion model demonstrated that there is a substantial inflammatory cell infiltrate into the subcutaneous tissue and into the tendon wound within 24 hours. After this time point, inflammatory cell numbers gradually decline. The vast majority of these were neutrophils, which appeared and rapidly disappeared within a 5 days. This suggests that with a clean, sharp focused injury, the neutrophil response is short. Proliferative activity Vital dye cells started in the ST at day 3 and gradually the activity spread into the tendon wound by day 7. Vital dye studies labeling sheath cells have shown that cells migrate into the tendon[33] and that tendon surface cells migrate into the tendon core[34] within 7 days in rabbit models. Peaks in F4/80 expression were observed in the subcutaneous tissue at days 3, 7, and 14. These observations were similar to those of Cowin et al[35] who observed peaks at day 3 and day 7 in healing skin wounds, and Kajikawa et al[36] who observed peaks at day 3 and 7 in patellar tendon wounds.

BrdU labeling also peaked at days 3 and 7 in the ST and on day 7, α-SMA expression was found to be very high as myofibroblasts and pericytes were seen in the wound. This marked the peak activity period in the ST and supports observations *in vitro* that tendon sheath cells have a propensity to express α-SMA whereas tendon fibroblasts do not in culture.[37]

On day 7, there is evidence of BrdU and Hsp47 staining in the damaged tendon, which gradually leads to peak in activity at day 21. During this time period, our ultrastructural observations identified two novel cell phenotypes with numerous cytoplasmic protrusions. One cell had large protrusions, containing large and small diameter fibrils. The other cell had small cytoplasmic protrusions containing small diameter fibrils. The latter cell phenotype bears some similarity to embryologic 'fibripositors' which

deposit collagen in parallel fibers, a phenotype that has not been seen in adult tendon until now.[23] This cell phenotype is likely to be involved in depositing new collagen as it coincides with peak levels of Hsp47 at this time point. The cell phenotype with protrusions containing large and small fibrils may have a phagocytosing role or have a role in realigning collagen, or coalescing smaller fibrils into larger fibrils. This does pose an interesting new area for the investigation of collagen trafficking, as the cells in the wound are quite different in morphology from those seen in embryonic tendon. Zavahir et al[38] also identified cells with long cytoplasmic protrusions in tendon wounds from day 5 to day 14 in a rat extensor tendon window model. From the spatial observations these cells are likely to be fibroblasts and macrophages, but there is the possibility that they are different parts of the same cell. Our findings were in keeping with those observed by Marsolais et al.[39] In their rat Achilles tendon model two peaks of ED 1+ systemic macrophages were observed, followed by a later ED 2+ local macrophage peak starting at day 14 and peaking at day 28. Evidence from green fluorescent protein bone marrow grafting studies suggests that bone marrow–derived cells that migrated into tendon wounds were mainly macrophages and had no role in collagen synthesis as measured by Hsp47.[36] This third peak of macrophages we observed may relate to macrophages migrating into the tendon substance once a bridge of adhesive tissue is formed. The precise role of F4/80 macrophages in tissue repair is not clear, but some studies have shown that they are present in tissues that undergo significant remodeling, such as endometrial tissue,[40] and F4/80 macrophages also appear to have a role in remodeling embryonic tissue following programmed cell death.[41] Studies have shown inhibiting the macrophage response in tendon, either leads to larger fibrils[42] or improved tendon architecture.[43] It would appear that the interactions between macrophages and collagen deposition in tendon merits closer inspection.

There was a gradual increasing number of cells undergoing apoptosis or cell death, peaking on day 84. Studies by Lui et al[44] characterized the apoptosis in patellar tendon wounds using TUNEL and caspase 3 antibodies and found that apoptosis occurred late in tendon healing with maximum expression around 28 days post-wounding. Our study appeared to show TUNEL expression and CD45 expressions were inversely associated. Furthermore the distribution of TUNEL and CD45+ cells in the tissues, on 3D cellular mapping, was similar. This association between inflammation and apoptosis is well described in skin wound studies, where apoptosis appears to have a role in removing inflammatory cells.[45] Moreover, the process of apoptosis appears to be an important process in tendon healing. Inhibition of p53 a key regulator of apoptotic activity in tendon has been shown to reduce apoptotic activity and delay the process of tendon healing.[46]

Few studies have addressed the healing biology of tendon and ST together in one study. Studies have shown that the tendon and sheath exhibit different matrix molecule profiles and growth factor profiles during flexor tendon healing.[47] Furthermore, the expression levels of the inflammatory messengers interleukin-1beta, cox-2 and inducible nitric oxide synthase are greater in the tendon than in the sheath indicating that "the two tissues exhibit disparate temporal and qualitative patterns of gene expression."[47] In our study, the ST was always the site of greatest inflammatory, proliferative, synthetic, vascularization, and apoptotic activity. Only beyond day 21, did the tendon show a similar number of collagen synthetic molecules to the ST. Our study has shown a difference in the dynamics and spatial distribution of cells involved in the healing process and formation of adhesions between tendon and sheath. A latent period exists between the time of ST healing, as compared with the time when flexor tendons begin to heal. We hypothesize that this latent period is less for extrasynovial tendon, based on the observations by Kajikawa et al.[36] This group observed that cell proliferation and collagen synthesis arose earlier in accordance with ST healing. This latent period could potentially be targeted for the biopharmaceutical manipulation of intrasynovial flexor tendon healing. The ST healing time may be accelerated to restore the gliding surfaces before healing of the tendon begins.

The use of 3D cellular mapping has proved invaluable in this study. Three dimensional modeling of tissues and mapping of cells along with the ability to make objects translucent, allow for a new appreciation of the cellular activity. Previous studies using Reconstruct have involved modeling of ultrastructural images.[22] In the past we have used Reconstruct on serial sectioned histological mouse tissue.[11] In this study we have further evolved the technique to include mapping of cell expression using a number of antibody markers. The 3D mapping of cells using this technique is only limited by the antibodies available and could prove to be a useful tool in investigating a large number of cellular markers. Furthermore this technique could be used to look in conjunction with other techniques, such as *in situ* hybridization or cell tracking or a combination of strategies, to model complex processes into a virtual environment.

Fundamentally, the interactions between the damaged tissues are complex. Potenza's[48] observations may be relevant, in that cells migrate into the tendon wound from the surrounding tissue, and evidence suggests circulating cells contribute to tendon healing as well.[36] However it appears blood vessel in growth through adhesions is not a prerequisite for intrasynovial tendon healing. Interestingly, Matthews et al[49] highlighted that intrinsic cell populations can heal tendon without adhesions. In an artificial environment where tendon is isolated from healing to other tissues this concept holds true, but in a trauma situation, where other structures are damaged achieving the differential healing without adhesions, is challenging. These concepts have their merits, however a more holistic approach to appreciating flexor tendon healing should be considered and the importance of the surrounding tissue interactions highlighted. The primitive mechanisms by which tissues repair after injury are indiscriminate to tissue types hence leading to fibrotic scarring.[50] When this involves two dynamic gliding tissue types such as tendon and sheath, the results are adhesions. This study aimed to produce an overview of the

process in the context of cellular pathobiology. The multicellular temporal and spatial expression involved in flexor tendon healing is far more complex than justified by intrinsic and extrinsic concepts of healing alone. With this new description of a murine model of flexor tendon healing, researchers are now better placed to further investigate the mechanism of multiple tissue healing dynamics. New methods by which we can improve on the tendon healing process may now be identified.

References

1. Caulfield RH, Maleki-Tabrizi A, Patel H, Coldham F, Mee S, Nanchahal J: Comparison of zones 1 to 4 flexor tendon repairs using absorbable and unabsorbable four-strand core sutures. J Hand Surg Eur Vol 2008, 33:412–417
2. Bunnell S: Tendons. Surgery of the Hand. London, Pitman Medical Publishing, 1956, pp 434–519
3. Verdan C: Chirurgie reparatrice et fonctionnelle des tendons de la main. Paris Expansion Scientifique Francaise, 1952, pp 174–176
4. Potenza AD: Critical evaluation of flexor tendon healing and adhesion formation within artificial flexor sheaths. J Bone Joint Surg Am 1963, 45:1217–1233
5. Matthews P, Richards H: Factors in the adherence of flexor tendon after repair: an experimental study in the rabbit. J Bone Joint Surg Br 1976, 58:230–236
6. Hansson HA, Lundborg G, Rydevik B: Restoration of superficially damaged flexor tendons in synovial environment. An experimental ultrastructural study in rabbits. Scand J Plast Reconstr Surg 1980, 14:109–114
7. Manske PR, Lesker PA: Histologic evidence of intrinsic flexor tendon repair in various experimental animals. An in vitro study. Clin Orthop 1984, 297–304
8. Lundborg G, Rank F, Heinau B: Intrinsic tendon healing. A new experimental model. Scand J Plast Reconstr Surg 1985, 19:113–117
9. Reid RR, Said HK, Mogford JE, Mustoe TA: The future of wound healing: pursuing surgical models in transgenic and knockout mice. J Am Coll Surg 2004, 199:578–585
10. Silver LM: Mouse Genetics- Concepts and Applications. Oxford University Press, 1995, pp 3–11
11. Wong J, Bennett W, Ferguson MW, McGrouther DA: Microscopic and histological examination of the mouse hindpaw digit and flexor tendon arrangement with 3D reconstruction. J Anat 2006, 209:533–545
12. Wong JK, Cerovac S, Ferguson MW, McGrouther DA: The cellular effect of a single interrupted suture on tendon. J Hand Surg [Br] 2006, 31:358–367
13. Hasslund S, Jacobson JA, Dadali T, Basile P, Ulrich-Vinther M, Soballe K, Schwarz EM, O'Keefe RJ, Mitten DJ, Awad HA: Adhesions in a murine flexor tendon graft model: autograft versus allograft reconstruction. J Orthop Res 2008, 26:824–833
14. Wojciak B, Crossan JF: The accumulation of inflammatory cells in synovial sheath and epitenon during adhesion formation in healing rat flexor tendons. Clin Exp Immunol 1993, 93:108–114
15. Branford OA, Mudera V, Brown RA, McGrouther DA, Grobbelaar AO: A novel biomimetic material for engineering postsurgical adhesion using the injured digital flexor tendon-synovial complex as an in vivo model. Plast Reconstr Surg 2008, 121:781–793
16. Garner WL, McDonald JA, Koo M, Kuhn C, III, Weeks PM: Identification of the collagen-producing cells in healing flexor tendons. Plast Reconstr Surg 1989, 83:875–879
17. Gelberman RH, Khabie V, Cahill CJ: The revascularization of healing flexor tendons in the digital sheath. A vascular injection study in dogs. J Bone Joint Surg Am 1991, 73:868–881
18. Khan U, Edwards JC, McGrouther DA: Patterns of cellular activation after tendon injury. J Hand Surg [Br] 1996, 21:813–820
19. Ross R: The fibroblast and wound repair. Biol Rev Camb Philos Soc 1968, 43:51–96
20. Beckstead JH: A simple technique for preservation of fixation-sensitive antigens in paraffin-embedded tissues. J Histochem Cytochem 1994, 42:1127–1134
21. Cruz-Orive LM: Precision of Cavalieri sections and slices with local errors. J Microsc 1999, 193:182–198
22. Fiala JC: Reconstruct: a free editor for serial section microscopy. J Microsc 2005, 218:52–61
23. Canty EG, Lu Y, Meadows RS, Shaw MK, Holmes DF, Kadler KE: Coalignment of plasma membrane channels and protrusions (fibripositors) specifies the parallelism of tendon. J Cell Biol 2004, 165:553–563
24. Bunnell S: Repair of tendons in the fingers. Surgery, gynecology, and obstetrics. 1922, 35:88–97
25. Guimberteau JC: How is the anatomy adopted for tendon sliding? New ideas in hand flexor tendon surgery. Bordeaux, Acuitaine Domaine Forestier, 2001, pp 47–90
26. Chang J, Thunder R, Most D, Longaker MT, and Lineaweaver WC: Studies in flexor tendon wound healing: neutralizing antibody to TGF-beta1 increases postoperative range of motion. Plast Reconstr Surg 2000, 105:148–155
27. Bates SJ, Morrow E, Zhang AY, Pham H, Longaker MT, Chang J: Mannose-6-phosphate, an inhibitor of transforming growth factor-beta, improves range of motion after flexor tendon repair. J Bone Joint Surg Am 2006, 88:2465–2472
28. Lindsay WK, Thomson HG: Digital flexor tendons: an experimental study. Part I. The significance of each component of the flexor mechanismhin tendon healing. Br J Plast Surg 1960, 12:289–316
29. Akali A, Khan U, Khaw PT, McGrouther AD: Decrease in adhesion formation by a single application of 5-fluorouracil after flexor tendon injury. Plast Reconstr Surg 1999, 103:151–158
30. Bishop AT, Cooney WP, III, Wood MB: Treatment of partial flexor tendon lacerations: the effect of tenorrhaphy and early protected mobilization. J Trauma 1986, 26:301–312
31. Kubota H, Manske PR, Aoki M, Pruitt DL, Larson BJ: Effect of motion and tension on injured flexor tendons in chickens. J Hand Surg [Am] 1996, 21:456–463
32. Small JO, Brennen MD, Colville J: Early active mobilisation following flexor tendon repair in zone 2. J Hand Surg [Br] 1989, 14:383–391
33. Harrison RK, Mudera V, Grobbelaar AO, Jones ME, McGrouther DA: Synovial sheath cell migratory response to flexor tendon injury: an experimental study in rats. J Hand Surg [Am] 2003, 28:987–993
34. Jones ME, Mudera V, Brown RA, Cambrey AD, Grobbelaar AO, McGrouther DA: The early surface cell response to flexor tendon injury. J Hand Surg [Am] 2003, 28:221–230
35. Cowin AJ, Holmes TM, Brosnan P, Ferguson MW: Expression of TGF-beta and its receptors in murine fetal and adult dermal wounds. Eur J Dermatol 2001, 11:424–431
36. Kajikawa Y, Morihara T, Sakamoto H, Matsuda K, Oshima Y, Yoshida A, Nagae M, Arai Y, Kawata M, Kubo T: Platelet-rich plasma enhances the initial mobilization of circulation-derived cells for tendon healing. J Cell Physiol 2008, 215:837–845
37. Ragoowansi R, Khan U, Brown RA, McGrouther DA: Differences in morphology, cytoskeletal architecture and protease production between zone II tendon and synovial fibroblasts in vitro. J Hand Surg [Br] 2003, 28:465–470
38. Zavahir F, McGrouther DA, Misra A, Smith K, Brown RA, Mudera V: A study of the cellular response to orientated fibronectin material in healing extensor rat tendon. J Mater Sci Mater Med 2001, 12:1005–1011
39. Marsolais D, Cote CH, Frenette J: Neutrophils and macrophages accumulate sequentially following Achilles tendon injury. J Orthop Res 2001, 19:1203–1209
40. Hudson SN, Seamark RF, Robertson SA: The effect of restricted nutrition on uterine macrophage populations in mice. J Reprod Immunol 1999, 45:31–48
41. Hopkinson-Woolley J, Hughes D, Gordon S, Martin P: Macrophage recruitment during limb development and wound healing in the embryonic and foetal mouse. J Cell Sci 1994, 107 (Pt 5):1159–1167
42. Alaseirlis DA, Li Y, Cilli F, Fu FH, Wang JH: Decreasing inflammatory response of injured patellar tendons results in increased collagen fibril diameters. Connect Tissue Res 2005, 46:12–17
43. Hays PL, Kawamura S, Deng XH, Dagher E, Mithoefer K, Ying L, Rodeo SA: The role of macrophages in early healing of a tendon graft in a bone tunnel. J Bone Joint Surg Am 2008, 90:565–579
44. Lui PP, Cheuk YC, Hung LK, Fu SC, Chan KM: Increased apoptosis at the late stage of tendon healing. Wound Repair Regen 2007, 15:702–707
45. Brown DL, Kao WW, Greenhalgh DG: Apoptosis down-regulates in-

flammation under the advancing epithelial wound edge: delayed patterns in diabetes and improvement with topical growth factors. Surgery 1997, 121:372–380
46. Marsolais D, Cote CH, Frenette J: Pifithrin-alpha, an inhibitor of p53 transactivation, alters the inflammatory process and delays tendon healing following acute injury. Am J Physiol Regul Integr Comp Physiol 2007, 292:R321–R327
47. Berglund M, Reno C, Hart DA, Wiig M: Patterns of mRNA expression for matrix molecules and growth factors in flexor tendon injury: differences in the regulation between tendon and tendon sheath. J Hand Surg [Am] 2006, 31:1279–1287
48. Potenza AD: Detailed evaluation of healing processes in canine flexor digital tendons. Mil Med 1962, 127:34–47
49. Matthews P, Richards H: The repair reaction of flexor tendon within the digital sheath. Hand 1975, 7:27–29
50. Ferguson MW, O'Kane S: Scar-free healing: from embryonic mechanisms to adult therapeutic intervention. Philos Trans R Soc Lond B Biol Sci 2004, 359:839–850